University of Hertfordshire UH

SPINS-UK Meeting,
September 11th, 2024

Superfluid Spin-up: 3D Simulations of Post-Glitch Dynamics in Neutron Star Cores

arXiv:2407.18810

Dr Vanessa Graber
v.graber@herts.ac.uk

in collaboration with J. Rafael Fuentes
(University of Colorado Boulder)

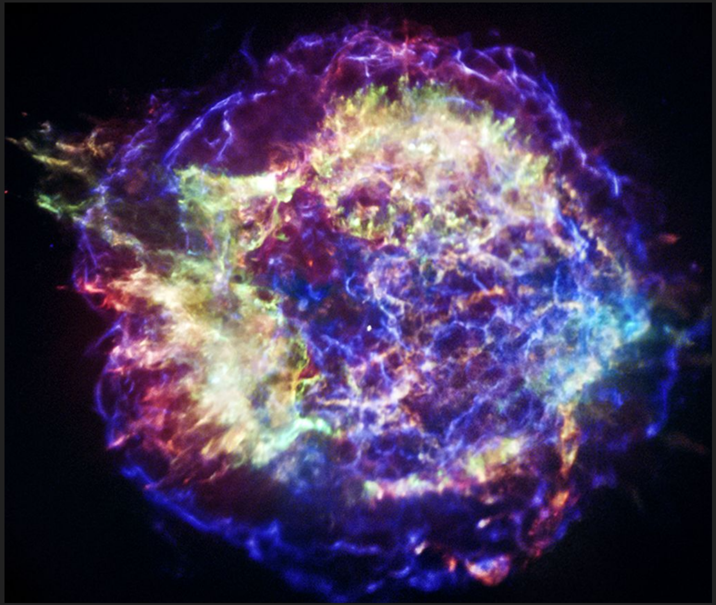

Cassiopeia A supernova remnant
(credit: NASA/CXC/SAO)

Neutron star interiors

- The interior structure of neutron stars is complex and influenced by the (unknown) nuclear-matter equation of state.

Neutron star interiors

- The interior structure of neutron stars is complex and influenced by the (unknown) nuclear-matter equation of state.

After ~10^4 yrs interior temperatures reach ~10^6 - 10^8 K.

Their structure is layered very much like the Earth.

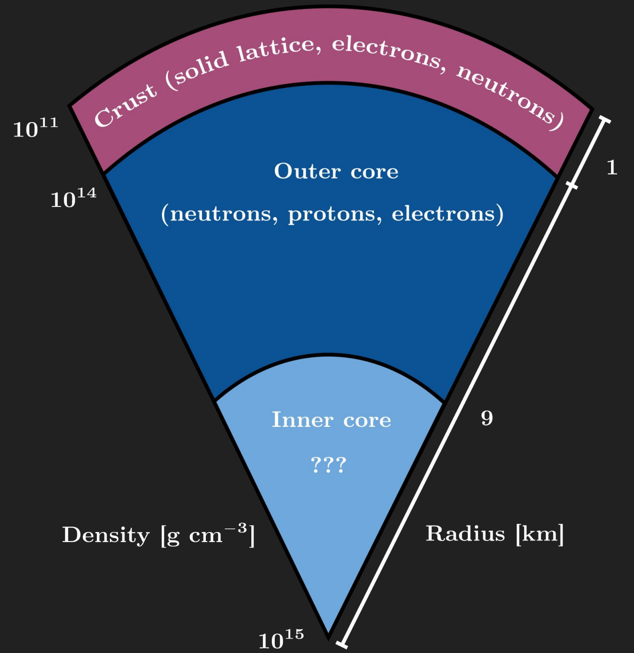

University of Hertfordshire UH

v.graber@herts.ac.uk

Neutron star interiors

- The interior structure of neutron stars is complex and influenced by the (unknown) nuclear-matter equation of state.

After ~10^4 yrs interior temperatures reach ~10^6 - 10^8 K.

Their structure is layered very much like the Earth.

We can decompose neutron stars into solid crusts and fluid cores.

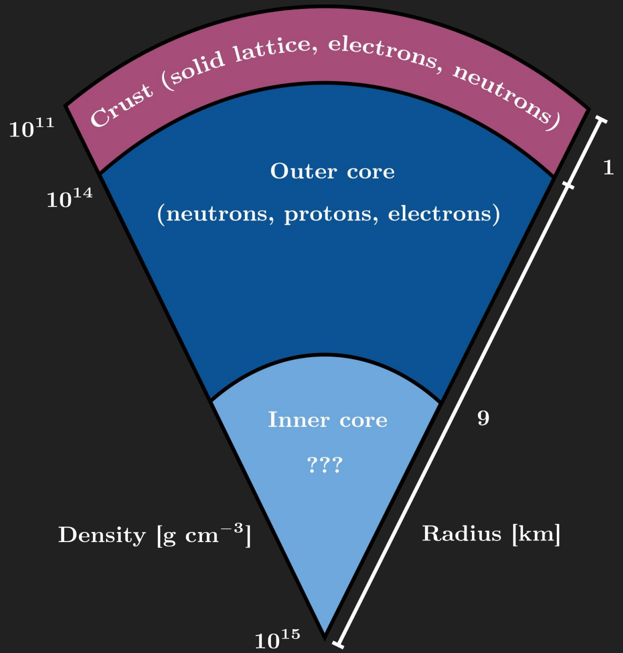

Superfluid components

- Although neutron stars are hot compared to laboratory experiments, they are cold in terms of their extremely high densities.

Interiors are well below neutron and proton Fermi temperatures ($\sim 10^{12}$ K).

Superfluid components

- Although neutron stars are hot compared to laboratory experiments, they are cold in terms of their extremely high densities.

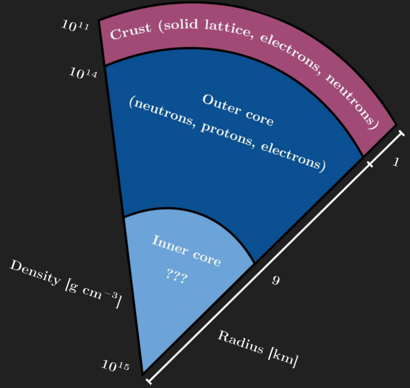

Interiors are well below neutron and proton Fermi temperatures (~10^{12} K).

Below a critical temperature T_c the fermionic nucleons can form Cooper pairs.

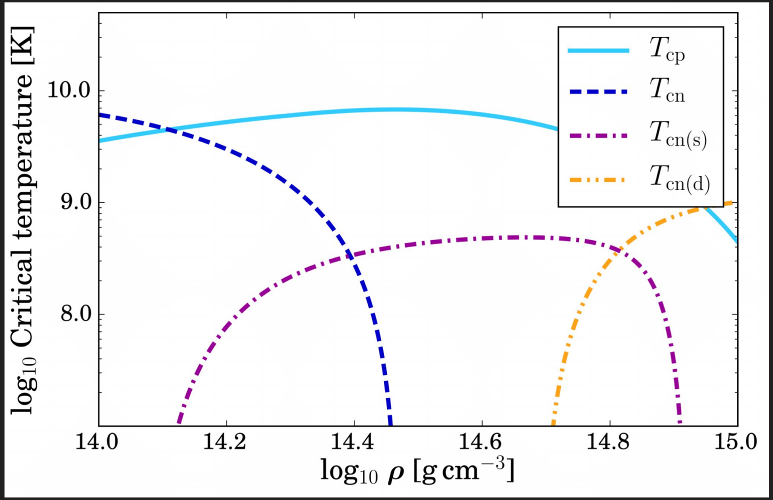

Superfluid components

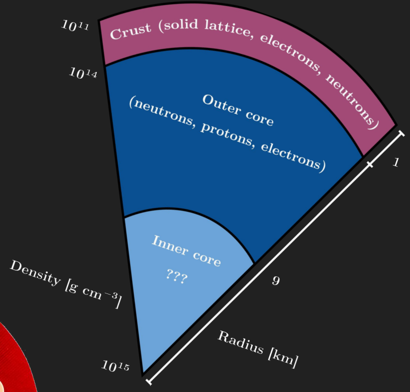

- Although neutron stars are hot compared to laboratory experiments, they are cold in terms of their extremely high densities.

Interiors are well below neutron and proton Fermi temperatures (~10^{12} K).

Below a critical temperature T_c the fermionic nucleons can form Cooper pairs.

Neutron stars contain at least 3 superfluid components.

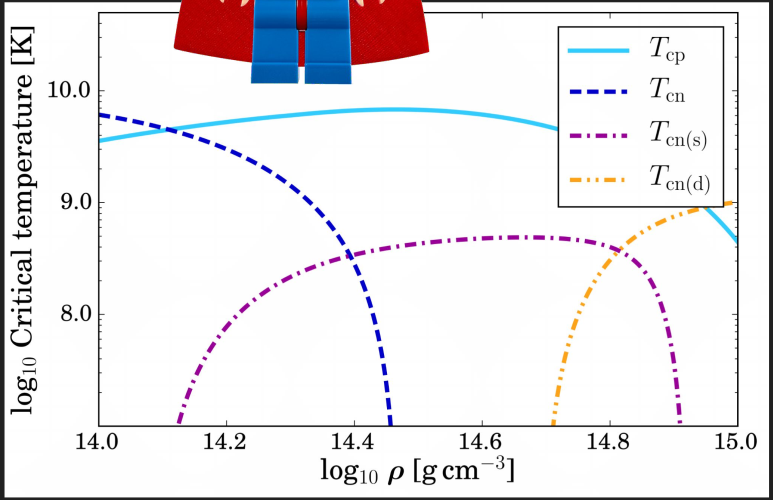

v.graber@herts.ac.uk

Quantum vortices

- Superfluids are macroscopic quantum states, characterised by a wave function $\Psi=\Psi_0 e^{i\varphi}$, which satisfies the Schrödinger equation.

Quantum vortices

- Superfluids are macroscopic quantum states, characterised by a wave function $\Psi = \Psi_0 e^{i\varphi}$, which satisfies the Schrödinger equation.

$\mathbf{v}_{SF} = \hbar / m_c \nabla \varphi$ dictates $\boldsymbol{\omega} = \nabla \times \mathbf{v}_{SF} = 0$. Superflow is irrotational.

Quantum vortices

Credit: NOAA Photo Library

- Superfluids are macroscopic quantum states, characterised by a wave function $\Psi=\Psi_0 e^{i\varphi}$, which satisfies the Schrödinger equation.

$\mathbf{v}_{SF} = \hbar/m_c \nabla \varphi$ dictates $\boldsymbol{\omega} = \nabla \times \mathbf{v}_{SF} = 0$. Superflow is irrotational.

SFs rotate by forming quantised vortices.

University of Hertfordshire UH

v.graber@herts.ac.uk

Quantum vortices

Credit: NOAA Photo Library

- Superfluids are macroscopic quantum states, characterised by a wave function $\Psi=\Psi_0 e^{i\varphi}$, which satisfies the Schrödinger equation.

$\mathbf{v}_{SF} = \hbar/m_c \nabla \varphi$ dictates $\boldsymbol{\omega} = \nabla \times \mathbf{v}_{SF} = 0$. Superflow is irrotational.

SFs rotate by forming quantised vortices.

Each vortex carries a quantum of circulation $\kappa = h/m_c$.

Quantum vortices

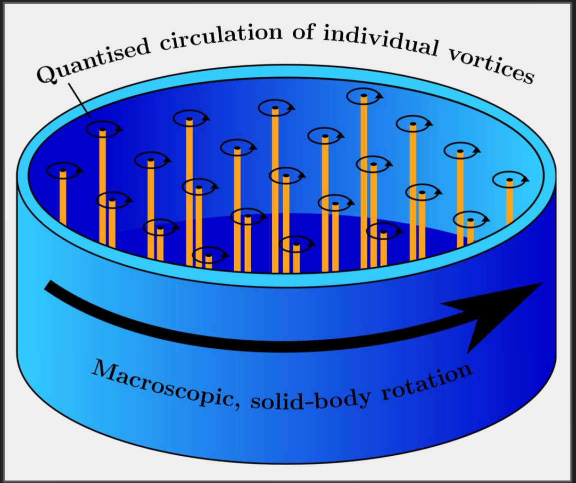

- Superfluids are macroscopic quantum states, characterised by a wave function $\Psi = \Psi_0 e^{i\varphi}$, which satisfies the Schrödinger equation.

$\mathbf{v}_{SF} = \hbar/m_c \nabla \varphi$ dictates $\boldsymbol{\omega} = \nabla \times \mathbf{v}_{SF} = 0$. Superflow is irrotational.

SFs rotate by forming quantised vortices.

Each vortex carries a quantum of circulation $\kappa = h/m_c$.

- The vortices form an array that mimics solid-body rotation on large scales $\omega = 2\Omega = N_v \kappa$.

Pulsar glitches I

- As observed by pulsar timing, the regular spin-down of neutron stars can be interrupted by sudden spin-ups.

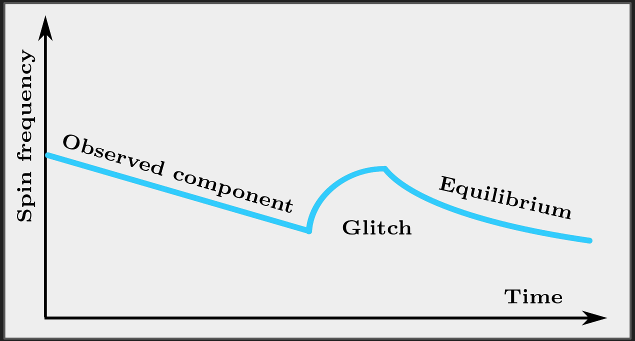

Pulsar glitches I

- As observed by pulsar timing, the regular spin-down of neutron stars can be interrupted by sudden spin-ups.

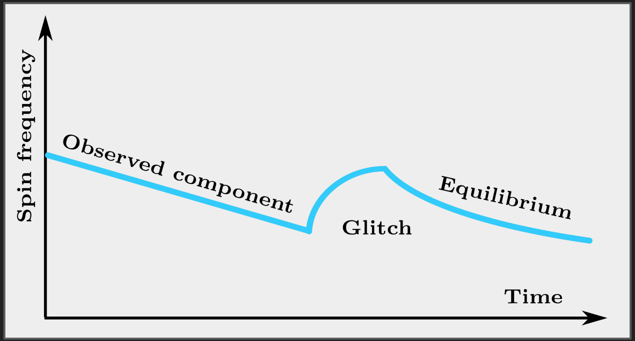

We can understand the glitch origin with an experiment.

Pulsar glitches I

- As observed by pulsar timing, the regular spin-down of neutron stars can be interrupted by sudden spin-ups.

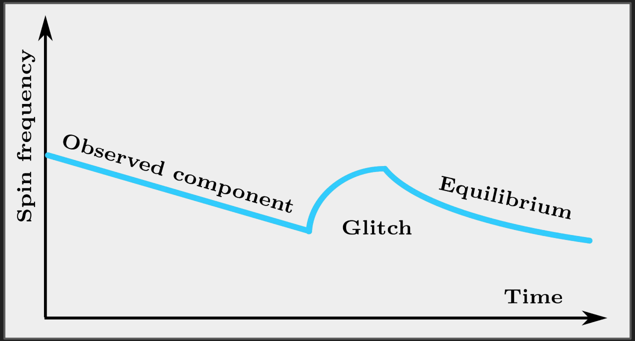

We can understand the glitch origin with an experiment.

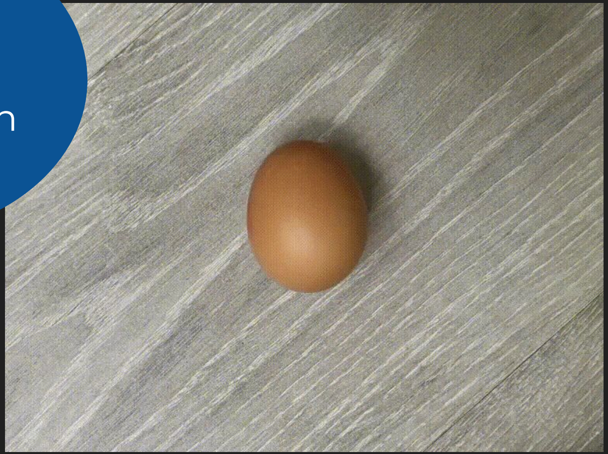

Pulsar glitches I

- As observed by pulsar timing, the regular spin-down of neutron stars can be interrupted by sudden spin-ups.

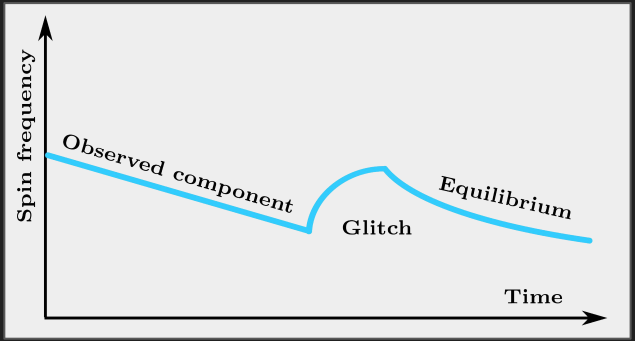

We can understand the glitch origin with an experiment.

cooked

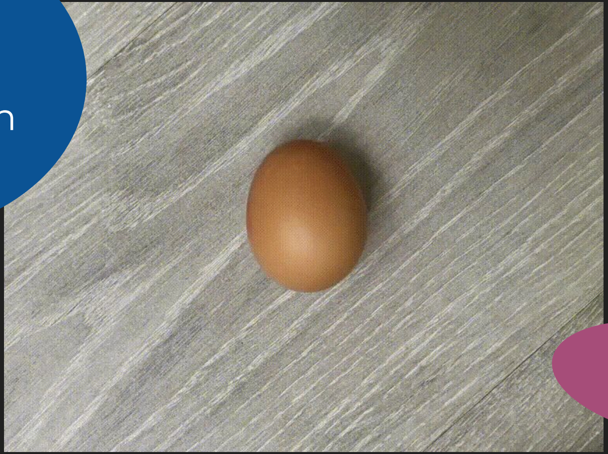

raw

Pular glitches II

- Spin-up glitches can be naturally explained in a multi-component neutron star model.

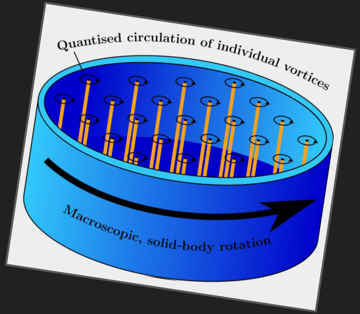

Superfluid spin-down can be impeded by pinning of vortices to crustal lattice.

Pular glitches II

- Spin-up glitches can be naturally explained in a multi-component neutron star model.

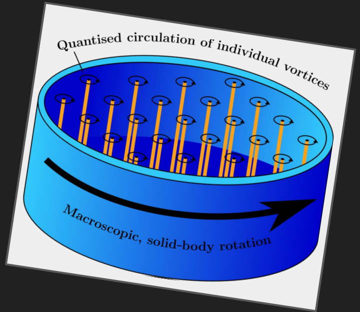

Superfluid spin-down can be impeded by pinning of vortices to crustal lattice.

The crustal superfluid acts as a reservoir of angular momentum.

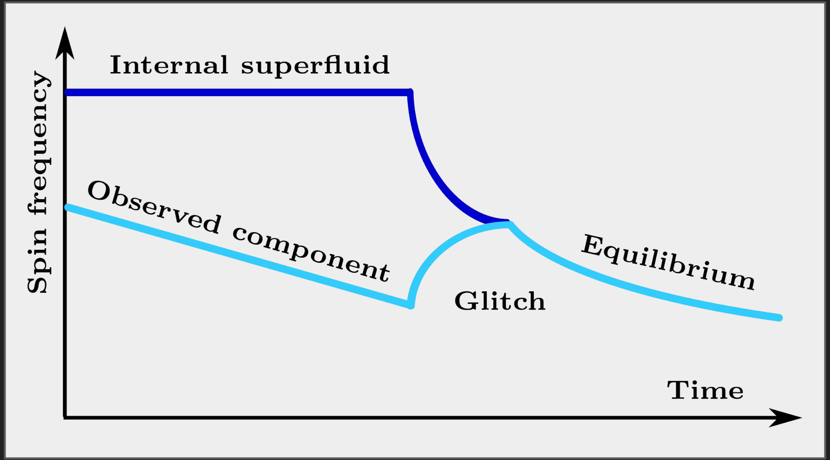

Pular glitches II

- Spin-up glitches can be naturally explained in a multi-component neutron star model.

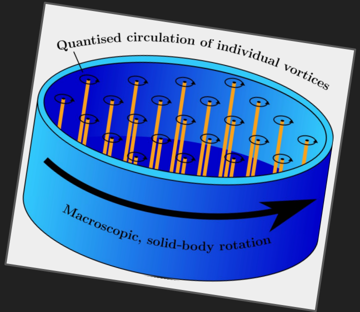

Superfluid spin-down can be impeded by pinning of vortices to crustal lattice.

The crustal superfluid acts as a reservoir of angular momentum.

The shape of the glitch encodes the (hidden) internal neutron star physics.

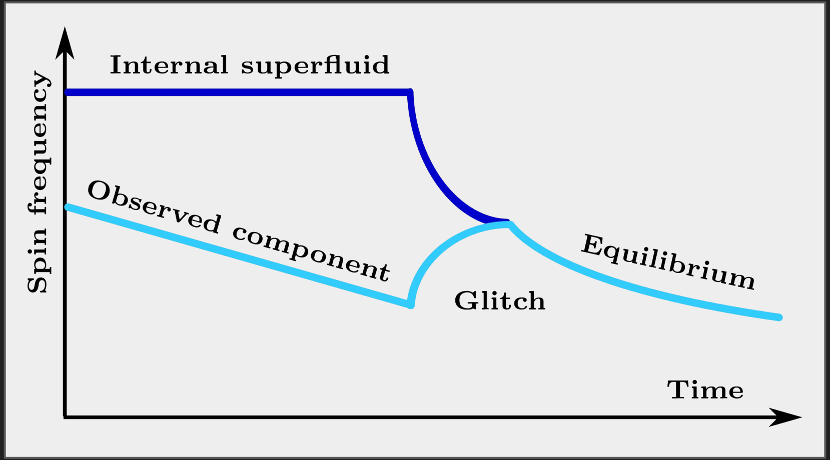

Numerical experiment set-up

- In our new study, we focus on the response of a two-component fluid core to a glitch that is driven by the crustal superfluid.

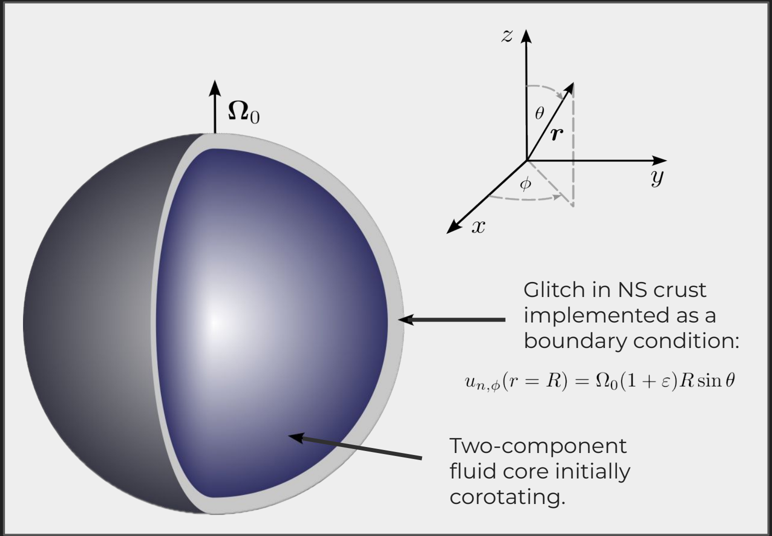

We model the NS crust as an infinitely thin boundary.

The core is modelled as superfluid (n) and a viscous (p and e⁻) mixture.

Numerical experiment set-up

- In our new study, we focus on the response of a two-component fluid core to a glitch that is driven by the crustal superfluid.

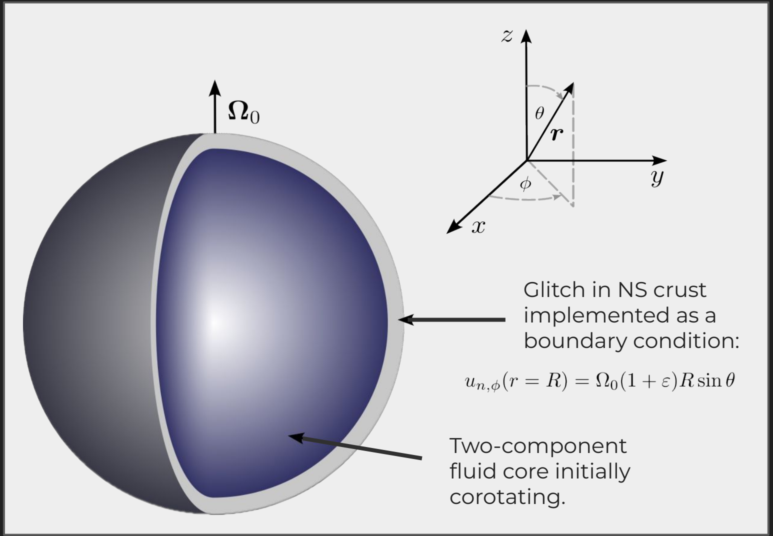

We model the NS crust as an infinitely thin boundary.

The core is modelled as superfluid (n) and a viscous (p and e^-) mixture.

At t=0, we increase the rotation rate of the viscous fluid at the boundary to $\Omega_0(1+\varepsilon)$ with $\varepsilon \sim 10^{-3}$.

Numerical experiment set-up

- In our new study, we focus on the response of a two-component fluid core to a glitch that is driven by the crustal superfluid.

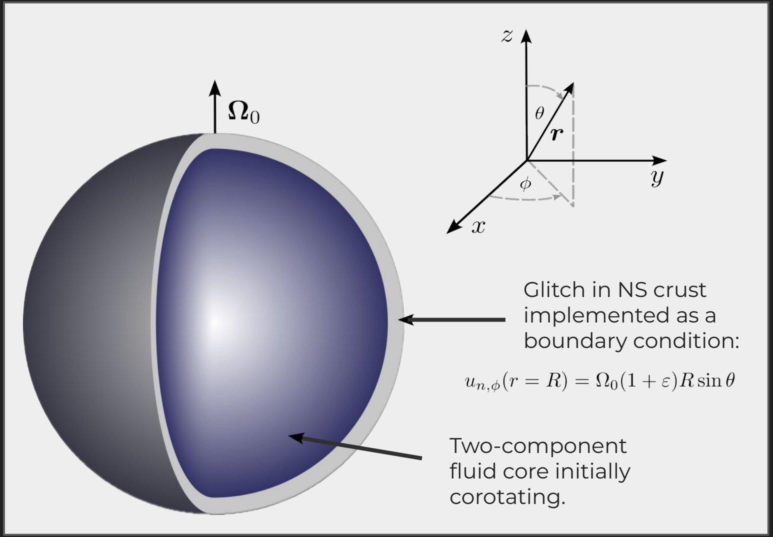

We model the NS crust as an infinitely thin boundary.

The core is modelled as superfluid (n) and a viscous (p and e^-) mixture.

At t=0, we increase the rotation rate of the viscous fluid at the boundary to $\Omega_0(1+\varepsilon)$ with $\varepsilon \sim 10^{-3}$.

Goal: Study the core's response to the glitch in full sphere for the first time.

HVBK Equations

- We focus on the hydrodynamical picture and solve the Hall–Vinen–Bekarevich–Khalatnikov (HVBK) equations initially developed for laboratory superfluid helium with the pseudo-spectral code Dedalus:

$$\frac{\partial \boldsymbol{u}_n}{\partial t} + \boldsymbol{u}_n \cdot \nabla \boldsymbol{u}_n = -\nabla \tilde{\mu}_n + \nu \nabla^2 \boldsymbol{u}_n + \frac{\boldsymbol{F}_{\rm MF}}{\rho_n} \,, \quad (1)$$

$$\frac{\partial \boldsymbol{u}_s}{\partial t} + \boldsymbol{u}_s \cdot \nabla \boldsymbol{u}_s = -\nabla \tilde{\mu}_s - \frac{\boldsymbol{F}_{\rm MF}}{\rho_s} \,, \quad (2)$$

$$\nabla \cdot \boldsymbol{u}_n = 0 = \nabla \cdot \boldsymbol{u}_s \,, \quad (3)$$

$\mathbf{u}_n$ and $\mathbf{u}_s$ denote the two fluid velocities and $\varrho_{n,s}$ the mass densities with $\varrho=\varrho_n+\varrho_s$.

HVBK Equations

- We focus on the hydrodynamical picture and solve the Hall–Vinen–Bekarevich–Khalatnikov (HVBK) equations initially developed for laboratory superfluid helium with the pseudo-spectral code Dedalus:

$$\frac{\partial \boldsymbol{u}_n}{\partial t} + \boldsymbol{u}_n \cdot \boldsymbol{\nabla} \boldsymbol{u}_n = -\boldsymbol{\nabla} \tilde{\mu}_n + \nu \boldsymbol{\nabla}^2 \boldsymbol{u}_n + \frac{\boldsymbol{F}_{\mathrm{MF}}}{\rho_n} , \qquad (1)$$

$$\frac{\partial \boldsymbol{u}_s}{\partial t} + \boldsymbol{u}_s \cdot \boldsymbol{\nabla} \boldsymbol{u}_s = -\boldsymbol{\nabla} \tilde{\mu}_s - \frac{\boldsymbol{F}_{\mathrm{MF}}}{\rho_s} , \qquad (2)$$

$$\boldsymbol{\nabla} \cdot \boldsymbol{u}_n = 0 = \boldsymbol{\nabla} \cdot \boldsymbol{u}_s , \qquad (3)$$

$\mathbf{u}_n$ and $\mathbf{u}_s$ denote the two fluid velocities and $\varrho_{n,s}$ the mass densities with $\varrho=\varrho_n+\varrho_s$.

ν is the kinematic viscosity of the normal fluid and $\mu_{n,s}$ the chemical potentials.

HVBK Equations

- We focus on the hydrodynamical picture and solve the Hall–Vinen–Bekarevich–Khalatnikov (HVBK) equations initially developed for laboratory superfluid helium with the pseudo-spectral code Dedalus:

$$\frac{\partial \boldsymbol{u}_n}{\partial t} + \boldsymbol{u}_n \cdot \boldsymbol{\nabla} \boldsymbol{u}_n = -\boldsymbol{\nabla}\tilde{\mu}_n + \nu \boldsymbol{\nabla}^2 \boldsymbol{u}_n + \frac{\boldsymbol{F}_{\rm MF}}{\rho_n} , \qquad (1)$$

$$\frac{\partial \boldsymbol{u}_s}{\partial t} + \boldsymbol{u}_s \cdot \boldsymbol{\nabla} \boldsymbol{u}_s = -\boldsymbol{\nabla}\tilde{\mu}_s - \frac{\boldsymbol{F}_{\rm MF}}{\rho_s} , \qquad (2)$$

$$\boldsymbol{\nabla} \cdot \boldsymbol{u}_n = 0 = \boldsymbol{\nabla} \cdot \boldsymbol{u}_s , \qquad (3)$$

$$\boldsymbol{F}_{\rm MF} = \rho_s \left[\mathcal{B} \left(\hat{\boldsymbol{\omega}}_s \times (\boldsymbol{\omega}_s \times \boldsymbol{u}_{sn}) \right) + \mathcal{B}' \left(\boldsymbol{\omega}_s \times \boldsymbol{u}_{sn} \right) \right] , \qquad (4)$$

with $\boldsymbol{u}_{sn} = \boldsymbol{u}_s - \boldsymbol{u}_n, \ \boldsymbol{\omega}_s = \boldsymbol{\nabla} \times \boldsymbol{u}_s$

$\mathbf{u}_n$ and $\mathbf{u}_s$ denote the two fluid velocities and $\varrho_{n,s}$ the mass densities with $\varrho=\varrho_n+\varrho_s$.

ν is the kinematic viscosity of the normal fluid and $\mu_{n,s}$ the chemical potentials.

$\mathbf{F}_{MF}$ is the mutual friction force due to interactions of vortices and their surroundings.

University of Hertfordshire UH
v.graber@herts.ac.uk

Characteristic time scales

- For realistic neutron stars, we estimate the mutual friction and Ekman timescale as follows:

$$\tau_{\rm MF} \sim \frac{1}{2\Omega_s \mathcal{B}} \sim 80\ {\rm s} \left(\frac{P_{\rm rot}}{0.1\ {\rm s}}\right) \left(\frac{\mathcal{B}}{10^{-4}}\right)^{-1}$$

For the scattering of electrons off of neutron vortices, we have $B \sim 10^{-4}$ and $B' \sim B^2$.

Characteristic time scales

- For realistic neutron stars, we estimate the mutual friction and Ekman timescale as follows:

$$\tau_{\rm MF} \sim \frac{1}{2\Omega_s \mathcal{B}} \sim 80\ {\rm s} \left(\frac{P_{\rm rot}}{0.1\ {\rm s}}\right) \left(\frac{\mathcal{B}}{10^{-4}}\right)^{-1}$$

$$\tau_{\rm Ek} \sim \frac{1}{\sqrt{\rm Ek}\,\Omega_n}$$ with $${\rm Ek} = \nu / 2\Omega_n R^2$$

$$\tau_{\rm Ek} \sim 10^3\ {\rm s} \left(\frac{x_n}{0.05}\right)^{-3/4} \left(\frac{\rho_n}{10^{14}\ {\rm g\ cm^{-3}}}\right)^{-1/4} \left(\frac{P_{\rm rot}}{0.1\ {\rm s}}\right)^{1/2} \left(\frac{T}{10^8\ {\rm K}}\right) \left(\frac{R}{10^6\ {\rm cm}}\right)$$

For electron-electron scattering, we have $v \sim 10^5 {\rm cm\ s}^2$ and ${\rm Ek} \sim 10^{-9}$.

For the scattering of electrons off of neutron vortices, we have $B \sim 10^{-4}$ and $B' \sim B^2$.

Characteristic time scales

- For realistic neutron stars, we estimate the mutual friction and Ekman timescale as follows:

$$\tau_{\mathrm{MF}} \sim \frac{1}{2\Omega_s \mathcal{B}} \sim 80\ \mathrm{s} \left(\frac{P_{\mathrm{rot}}}{0.1\ \mathrm{s}}\right) \left(\frac{\mathcal{B}}{10^{-4}}\right)^{-1}$$

$$\tau_{\mathrm{Ek}} \sim \frac{1}{\sqrt{\mathrm{Ek}}\Omega_n}$$ with $$\mathrm{Ek} = \nu / 2\Omega_n R^2$$

$$\tau_{\mathrm{Ek}} \sim 10^3\ \mathrm{s} \left(\frac{x_n}{0.05}\right)^{-3/4} \left(\frac{\rho_n}{10^{14}\ \mathrm{g\ cm^{-3}}}\right)^{-1/4} \left(\frac{P_{\mathrm{rot}}}{0.1\ \mathrm{s}}\right)^{1/2} \left(\frac{T}{10^8\ \mathrm{K}}\right) \left(\frac{R}{10^6\ \mathrm{cm}}\right)$$

For the scattering of electrons off of neutron vortices, we have $B \sim 10^{-4}$ and $B' \sim B^2$.

For electron-electron scattering, we have $\nu \sim 10^5\,\mathrm{cm\ s}^2$ and $\mathrm{Ek} \sim 10^{-9}$.

Note: Due to numerical constraints, we vary $B \sim 1\text{-}10^{-3}$ with $B/B' \sim 2$ and set $\mathrm{Ek} \sim 5\times10^{-3(4)}$.

Spinning up a single-component fluid I

- After the sudden spin-up, a thin boundary layer forms just below the crust and causes the bulk fluid to accelerate via Ekman pumping.

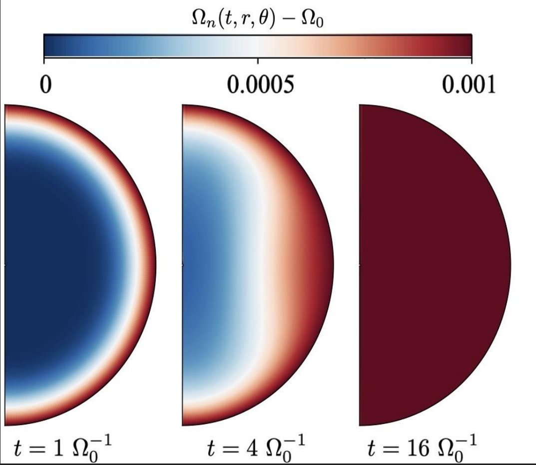

Spinning up a single-component fluid I

- After the sudden spin-up, a thin boundary layer forms just below the crust and causes the bulk fluid to accelerate via Ekman pumping.

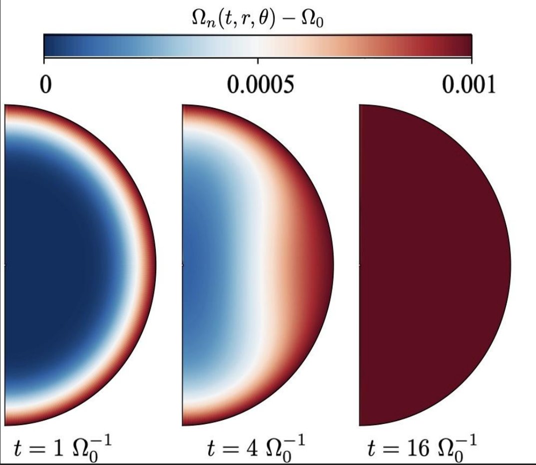

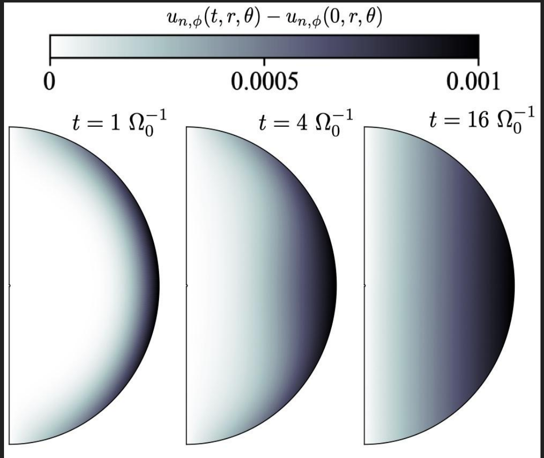

- As the evolution progresses, the azimuthal velocity becomes axisymmetric with constant magnitude over cylindrical surfaces.

Spinning up a single-component fluid I

- After the sudden spin-up, a thin boundary layer forms just below the crust and causes the bulk fluid to accelerate via Ekman pumping.

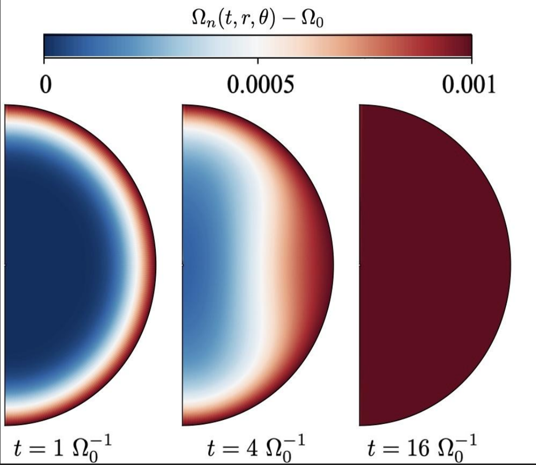

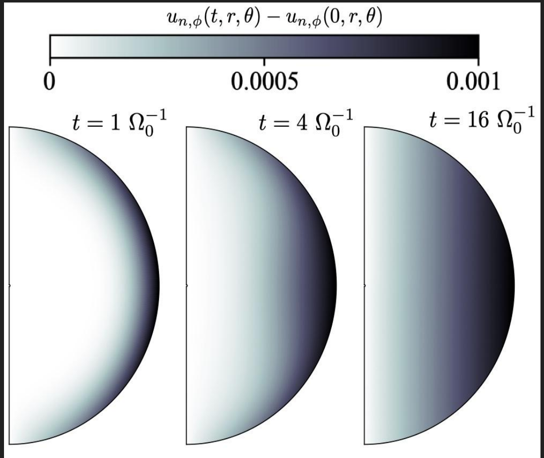

The axisymmetric behaviour is a direct result of the Taylor-Proudman theorem.

- As the evolution progresses, the azimuthal velocity becomes axisymmetric with constant magnitude over cylindrical surfaces.

Spinning up a single-component fluid II

- Ekman pumping leads to the formation of a stable circular flow pattern in each semi-hemisphere.

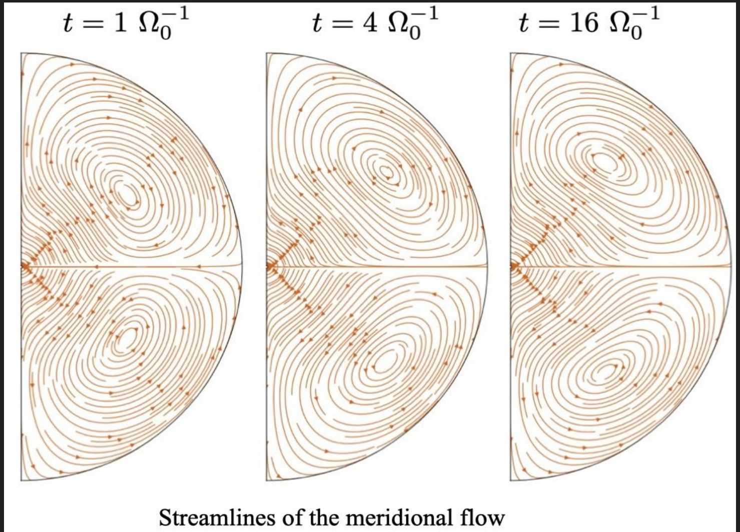

Spinning up a single-component fluid II

- Ekman pumping leads to the formation of a stable circular flow pattern in each semi-hemisphere.

As expected, a viscous fluid spins up on the Ekman time.

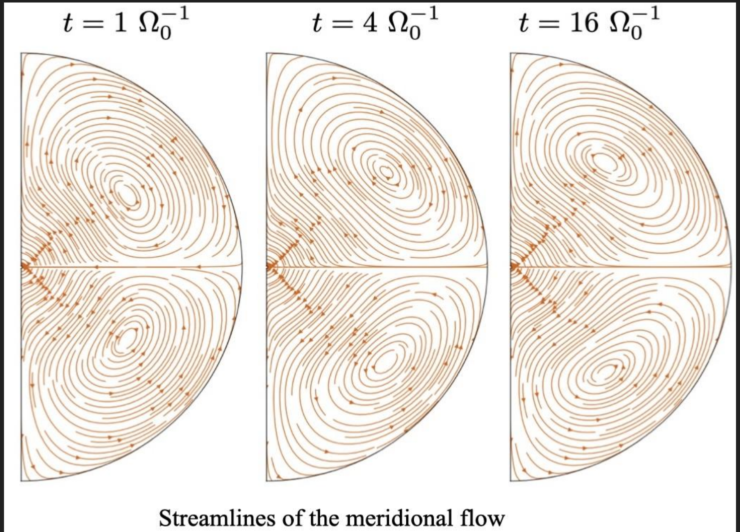

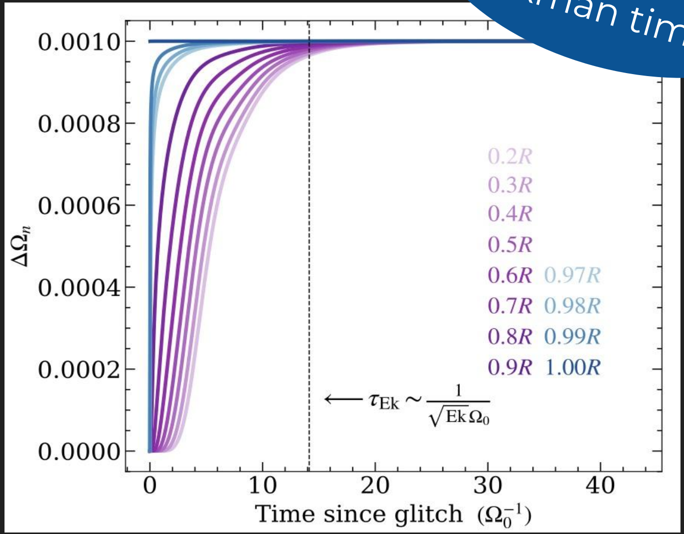

Spinning up a two-component fluid I

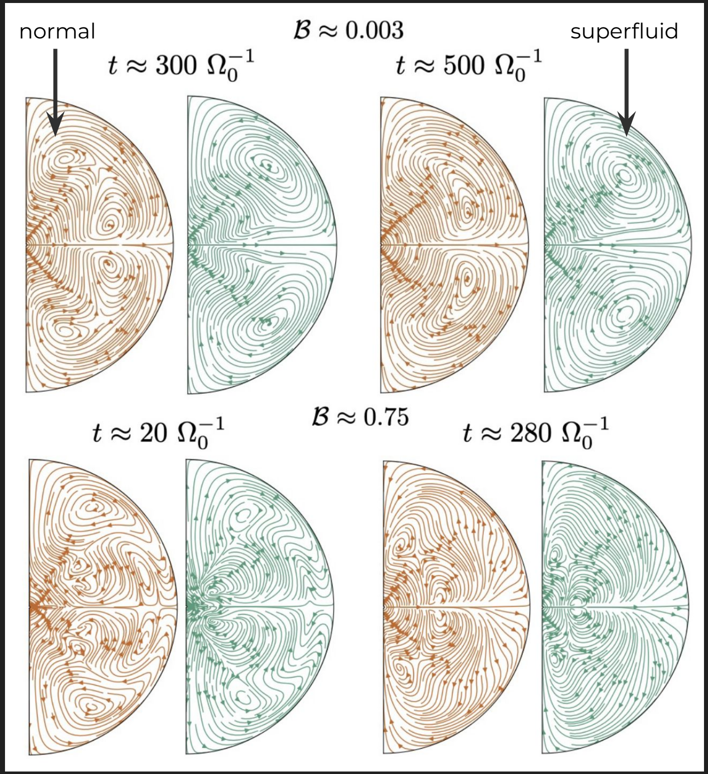

- The flow patterns look more complex than for the single-component case and we find similar patterns to earlier works in spherical shells (see Peralta et al. 2005, 2006, 2008).

Spinning up a two-component fluid I

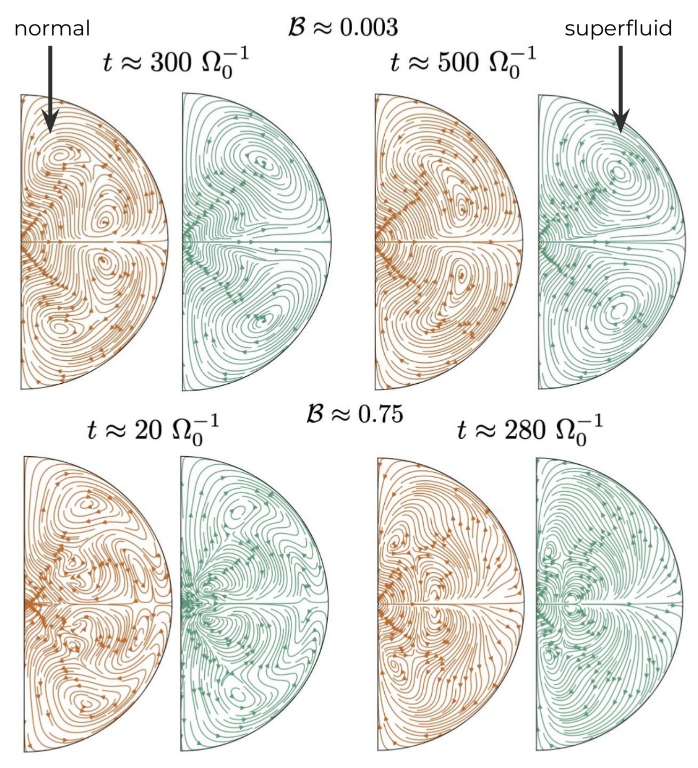

- The flow patterns look more complex than for the single-component case and we find similar patterns to earlier works in spherical shells (see Peralta et al. 2005, 2006, 2008).

In the weak coupling regime, the fluids seem to evolve almost independently.

For strong coupling, the superfluid follows the viscous fluid pattern.

Spinning up a two-component fluid I

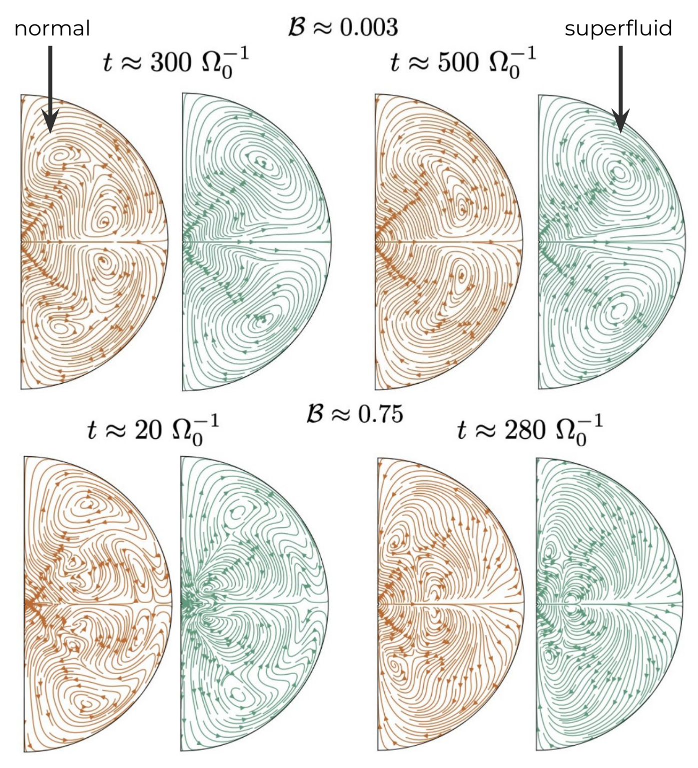

- The flow patterns look more complex than for the single-component case and we find similar patterns to earlier works in spherical shells (see Peralta et al. 2005, 2006, 2008).

In the weak coupling regime, the fluids seem to evolve almost independently.

For strong coupling, the superfluid follows the viscous fluid pattern.

For B~0.75, the normal fluid no longer develops the single cell flow structure.

Spinning up a two-component fluid II

- While the initial evolution is qualitatively similar and we obtain constant azimuthal velocities over cylindrical surfaces, the spin-up of the superfluid is delayed because of the mutual friction coupling.

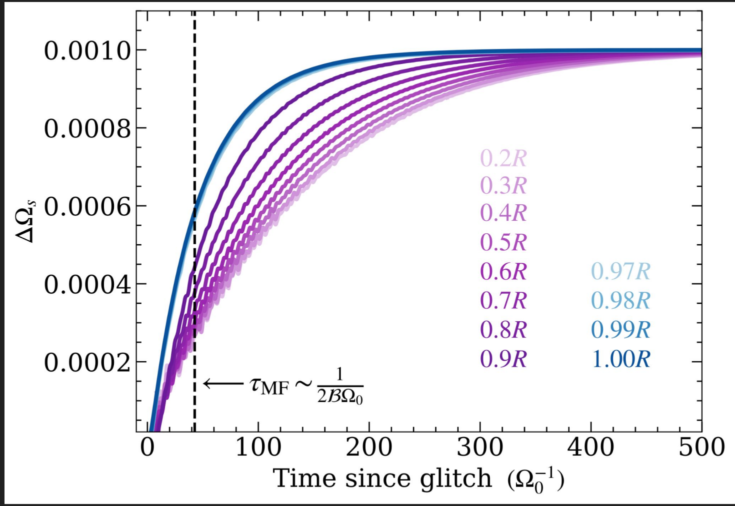

Spinning up a two-component fluid II

- While the initial evolution is qualitatively similar and we obtain constant azimuthal velocities over cylindrical surfaces, the spin-up of the superfluid is delayed because of the mutual friction coupling.

Superfluid can only accelerate once the Ekman pumping has spun up the viscous component.

Once differential rotation builds up, the superfluid is coupled via mutual friction.

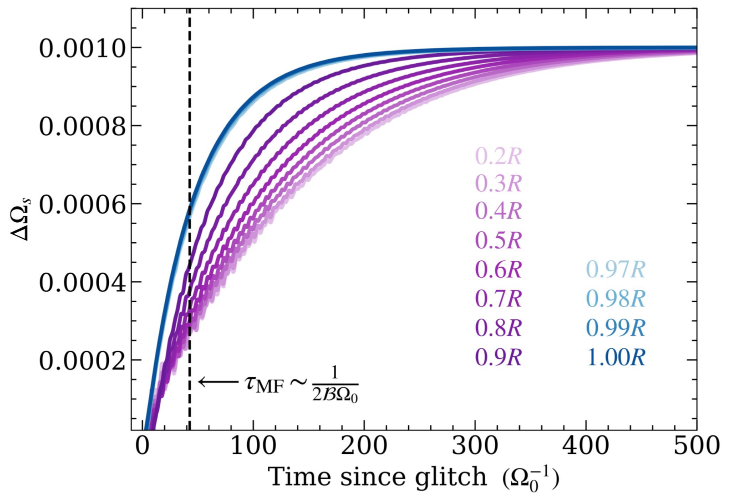

Spinning up a two-component fluid II

- While the initial evolution is qualitatively similar and we obtain constant azimuthal velocities over cylindrical surfaces, the spin-up of the superfluid is delayed because of the mutual friction coupling.

Superfluid can only accelerate once the Ekman pumping has spun up the viscous component.

Once differential rotation builds up, the superfluid is coupled via mutual friction.

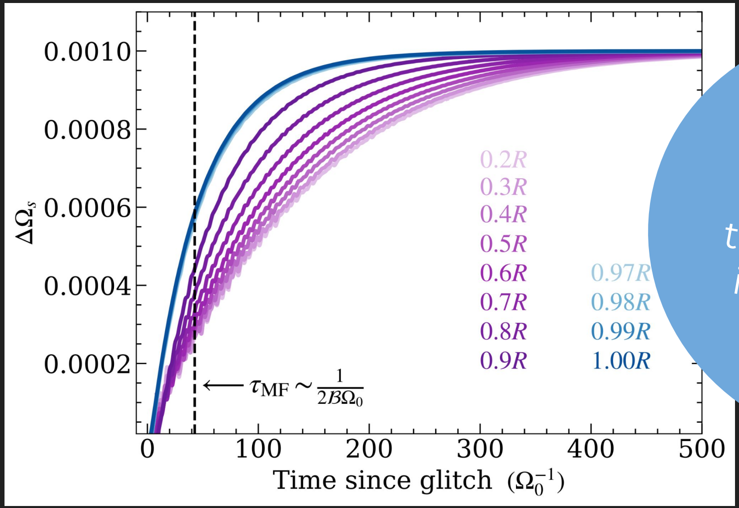

Outer superfluid layers spin up on the mutual friction timescale, while it takes longer for the inner layers.

v.graber@herts.ac.uk

Spinning up a two-component fluid III

- To extract the spin-up timescale, we fit $\Delta\Omega_s = \varepsilon(1 - e^{-t/t_{\text{spin-up}}})$

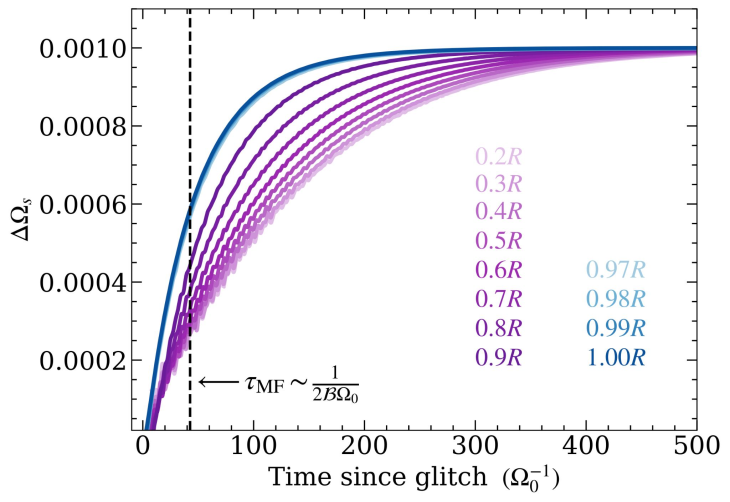

Spinning up a two-component fluid III

- To extract the spin-up timescale, we fit $$\Delta\Omega_s = \varepsilon(1 - e^{-t/t_{\text{spin-up}}})$$

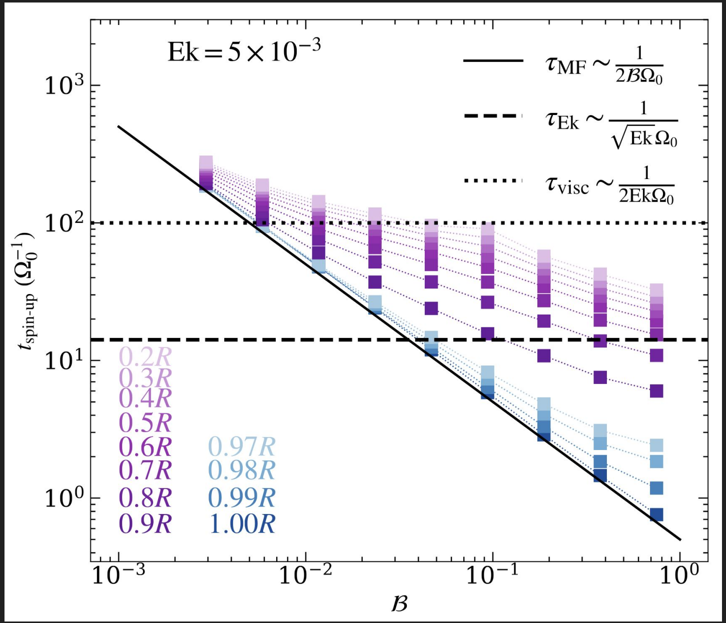

Spinning up a two-component fluid III

- To extract the spin-up timescale, we fit $\Delta\Omega_s = \varepsilon(1 - e^{-t/t_{\text{spin-up}}})$

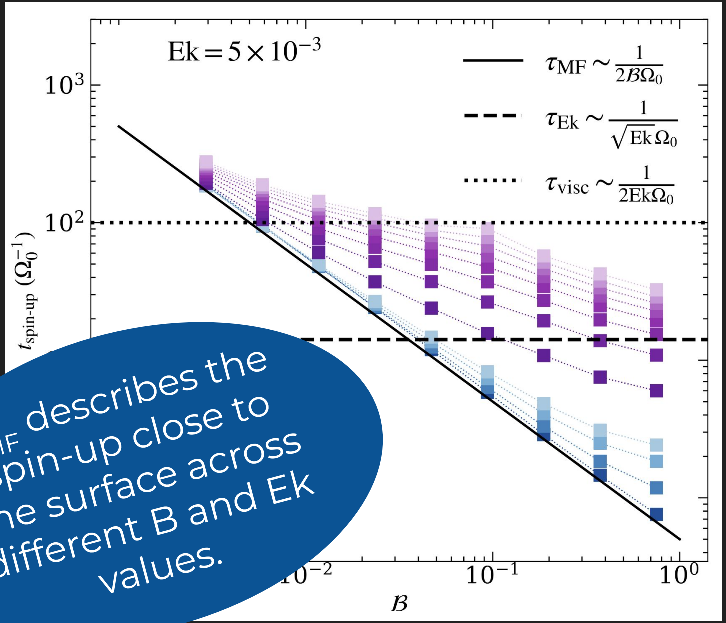

τ_MF describes the spin-up close to the surface across different B and Ek values.

Spinning up a two-component fluid III

- To extract the spin-up timescale, we fit

$$\Delta\Omega_s = \varepsilon\left(1 - e^{-t/t_{\rm spin-up}}\right)$$

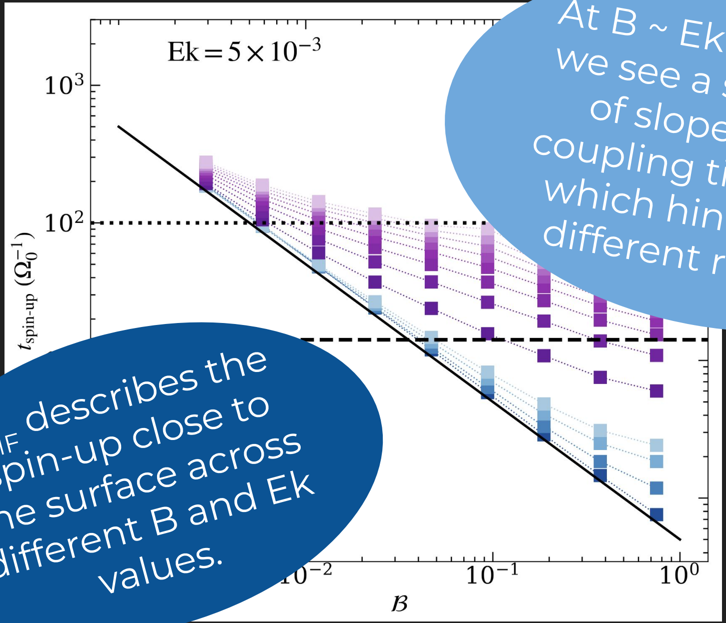

At B ~ $Ek^{0.5}$ (B~0.07), we see a separation of slopes in our coupling timescales, which hints at two different regimes.

τ_{MF} describes the spin-up close to the surface across different B and Ek values.

Spinning up a two-component fluid III

- To extract the spin-up timescale, we fit

$$\Delta\Omega_s = \varepsilon\left(1 - e^{-t/t_{\text{spin-up}}}\right)$$

$$t_{\text{spin-up}}(r) \approx C\tau_{\text{Ek}}^{\alpha}(\Delta R)\mathcal{B}^{-\gamma}$$

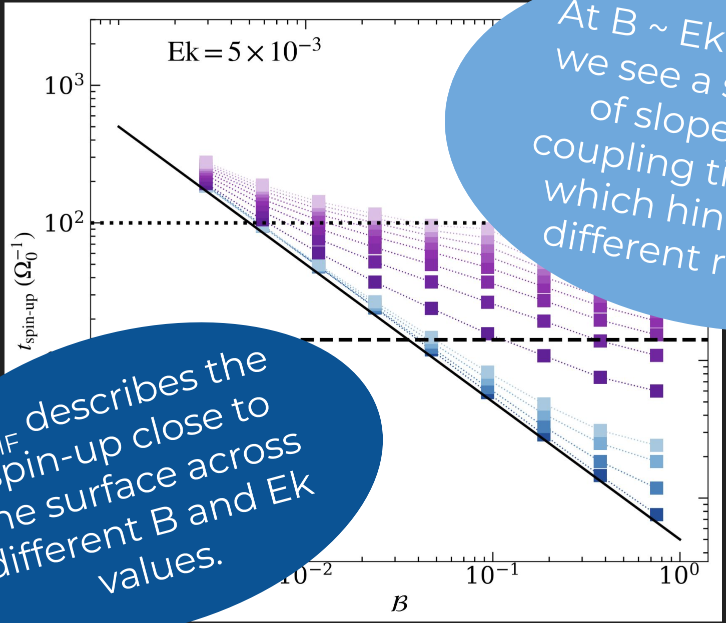

At B ~ Ek$^{0.5}$ (B~0.07), we see a separation of slopes in our coupling timescales, which hints at two different regimes.

τ_{MF} describes the spin-up close to the surface across the different B and Ek values.

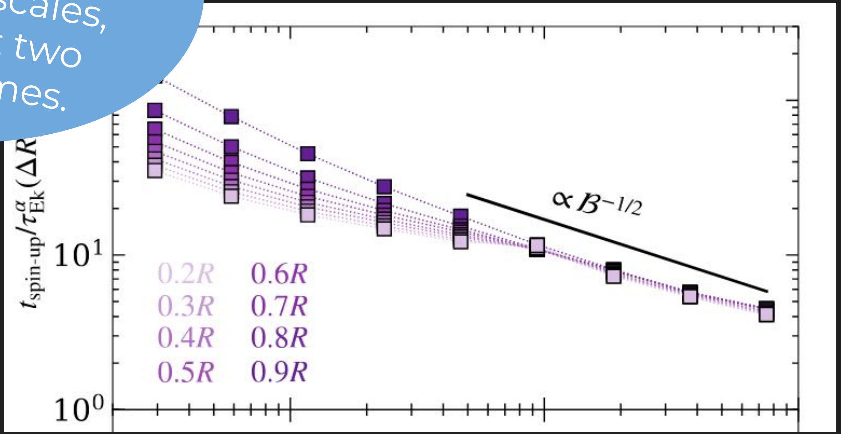

Spinning up a two-component fluid III

- To extract the spin-up timescale, we fit

$$\Delta\Omega_s = \varepsilon\left(1 - e^{-t/t_{\text{spin-up}}}\right)$$

$$t_{\text{spin-up}}(r) \approx C\tau_{\text{Ek}}^{\alpha}(\Delta R)\mathcal{B}^{-\gamma}$$

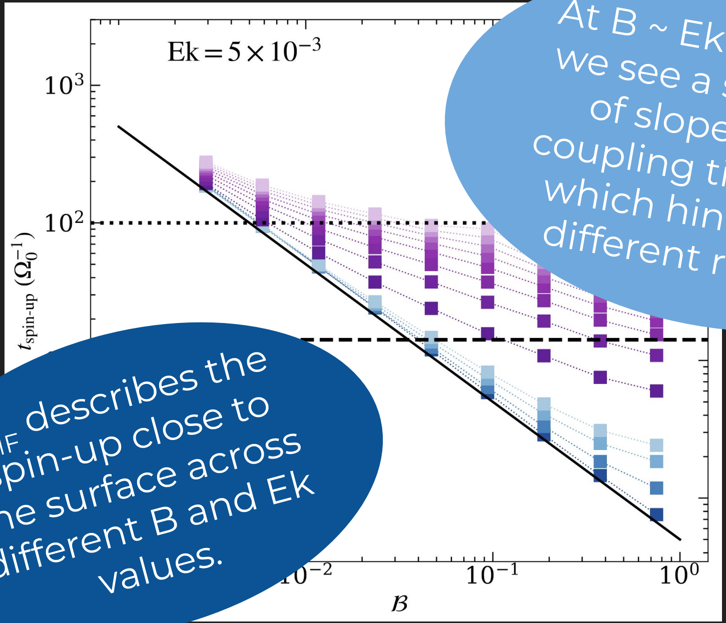

At B ~ $Ek^{0.5}$ (B~0.07), we see a separation of slopes in our coupling timescales, which hints at two different regimes.

τ_{MF} describes the spin-up close to the surface across the different B and Ek values.

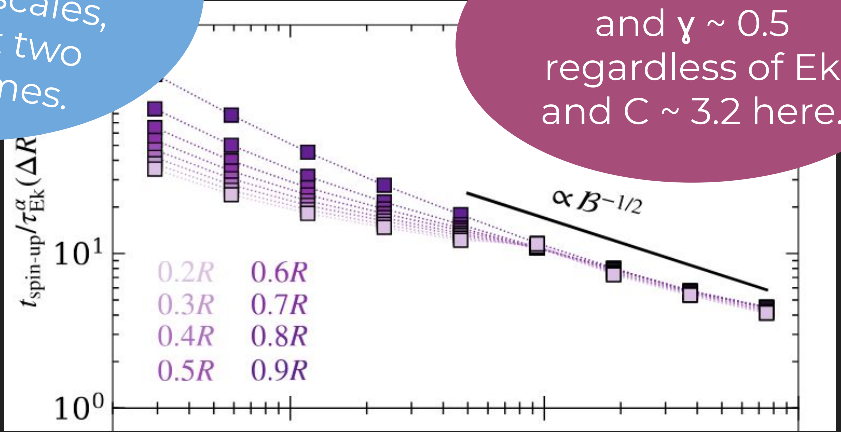

We find α ~ 0.85 and γ ~ 0.5 regardless of Ek and C ~ 3.2 here.

Conclusions & Outlook

Studying the shape of pulsar glitches, provides information on the hidden NS interior.

The spin-up of the outer SF layers is dominated by the mutual friction timescale. Inner layers show more complex behaviour.

We focused on the response of the spherical, two-component NS core following a glitch for the first time.

Conclusions & Outlook

Studying the shape of pulsar glitches, provides information on the hidden NS interior.

The spin-up of the outer SF layers is dominated by the mutual friction timescale. Inner layers show more complex behaviour.

We need to improve our treatment of the crust & study its response.

We still don't fully understand the coupling dynamics for low B values.

We focused on the response of the spherical, two-component NS core following a glitch for the first time.

Our simplified HVBK model neglects the presence of magnetic fields and non-constant densities.

THANK YOU

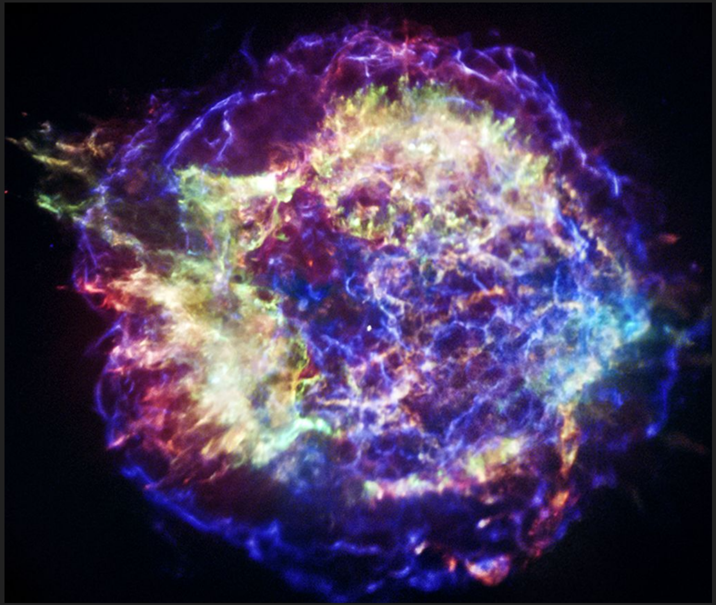

Cassiopeia A supernova remnant
(credit: NASA/CXC/SAO)

Some advertisement:

I will be joining **Royal Holloway** (University of London)'s growing Astronomy group in October on a Future Leaders Fellowship.

Positions open in the next few years on modelling **pulsar glitches and machine learning**:

2 PhD positions
3 Postdocs

Keep an eye open or come and talk to me if you want to learn more!

ROYAL HOLLOWAY UNIVERSITY OF LONDON

UK Research and Innovation

Superfluid Helium-4

- At low temperatures, helium-4 does not solidify but instead enters a new fluid phase.

The heat capacity resembles the Greek letter λ

Helium II behaviour has been explained by the two-fluid model.

Normal component: viscous properties and heat transport.

Inviscid component: SF features

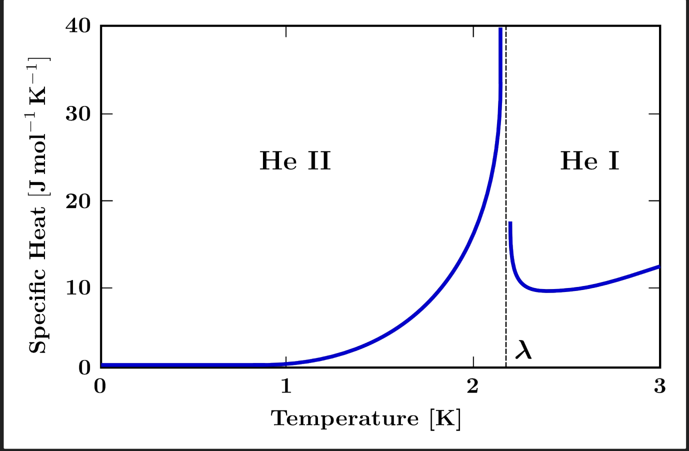

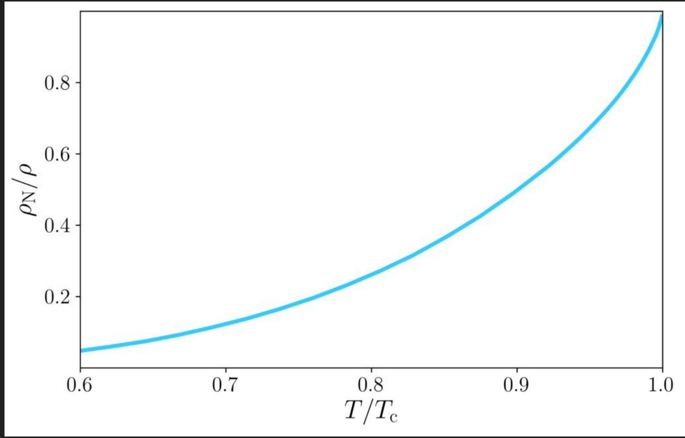

v.graber@herts.ac.uk

Mutual friction

- Although superfluids flow without friction, they can experience friction as a result of vortices interacting with their surroundings.

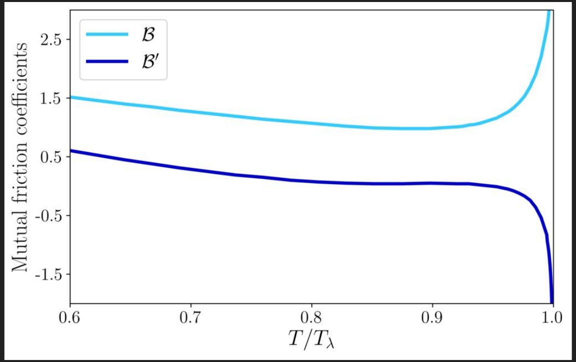

$$\mathbf{F}_{\rm mf} = \mathcal{B}_{\rm He} \frac{\rho_{\rm S}\rho_{\rm N}}{2\rho}\,\hat{\boldsymbol{\omega}}\times\left[\boldsymbol{\omega}\times(\mathbf{v}_{\rm S}-\mathbf{v}_{\rm N})-\frac{\mathbf{T}}{\rho_{\rm S}}\right] + \mathcal{B}'_{\rm He} \frac{\rho_{\rm S}\rho_{\rm N}}{2\rho}\left[\boldsymbol{\omega}\times(\mathbf{v}_{\rm S}-\mathbf{v}_{\rm N})-\frac{\mathbf{T}}{\rho_{\rm S}}\right]$$

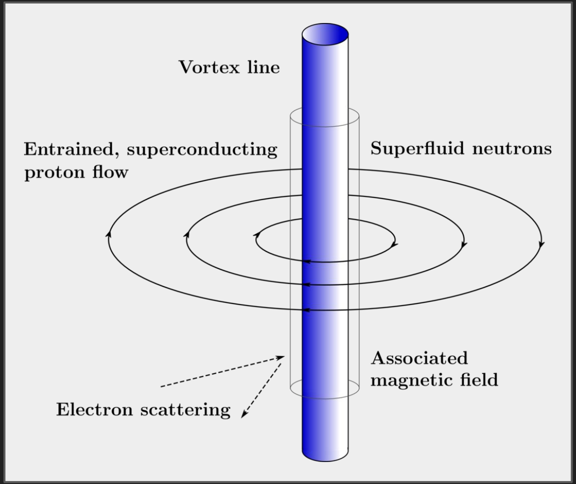

The two coefficients B/ B' determine the dissipation strength.

In helium II, the coefficients can be measured. For NSs, they need to be calculated.

v.graber@herts.ac.uk

Laboratory glitches

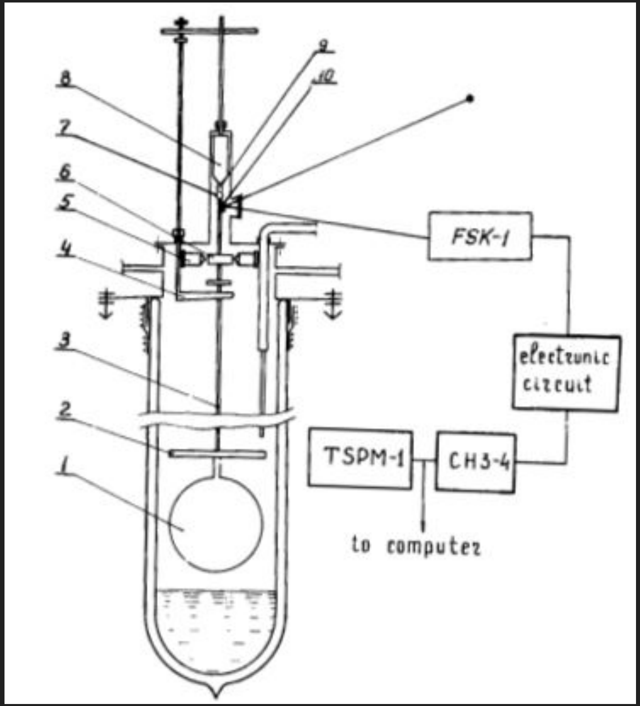

- In the 1970s, Tsakadze and Tsakadze performed the first (and only!!) systematic study of spin-up in helium II.

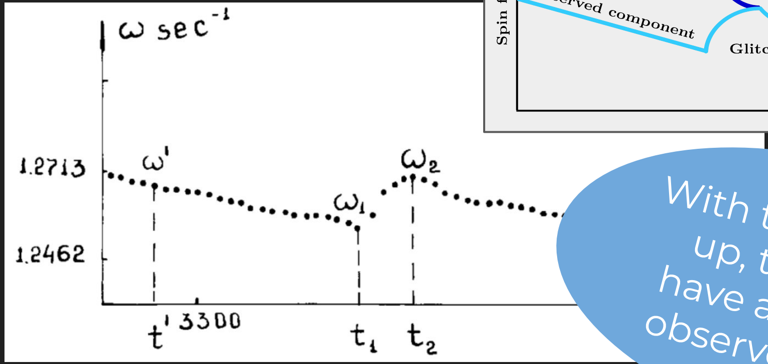

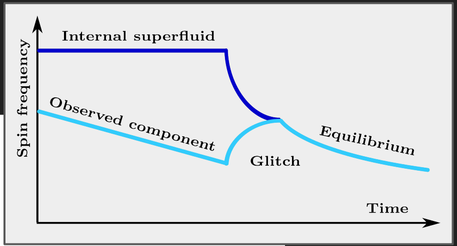

With their basic set up, they might have accidentally observed a glitch.

Credit: Tsakadze and Tsakadze (1980)

Spinning up a two-component fluid IV

- Spin-up timescales for two different Ekman numbers:

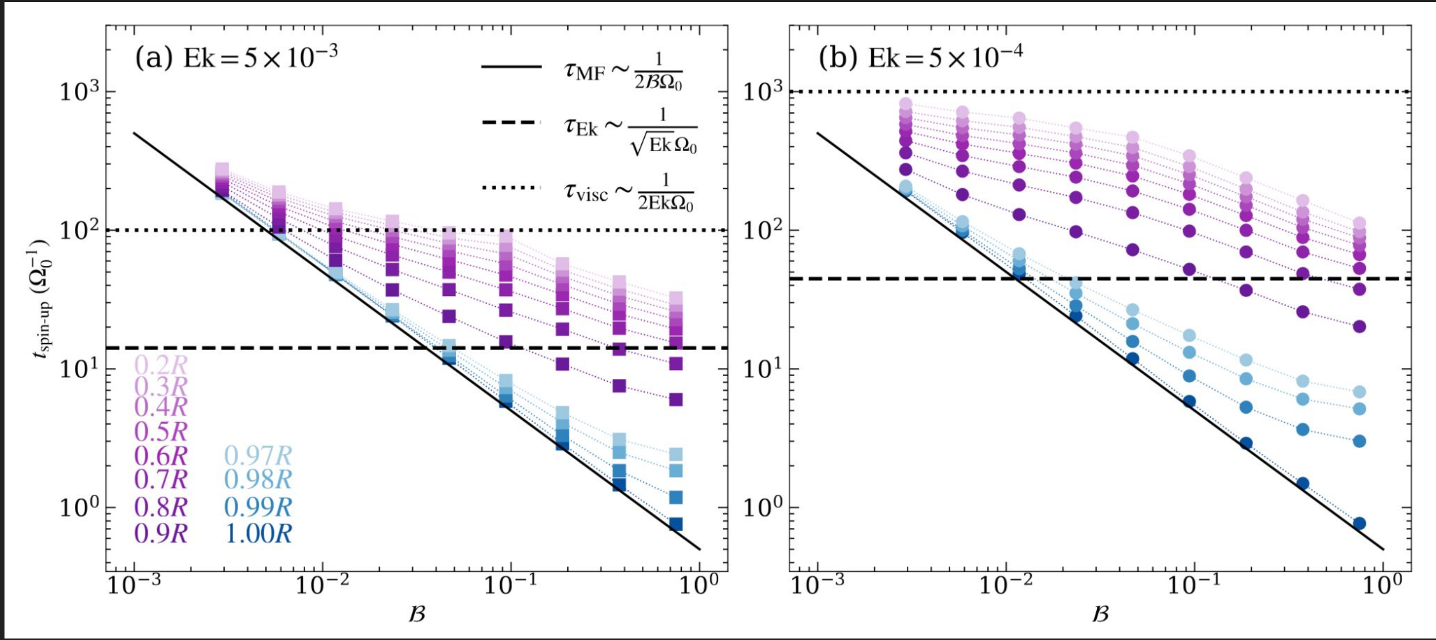

University of Hertfordshire UH

v.graber@herts.ac.uk

Spinning up a two-component fluid V

- Spin-up timescales for two different Ekman numbers:

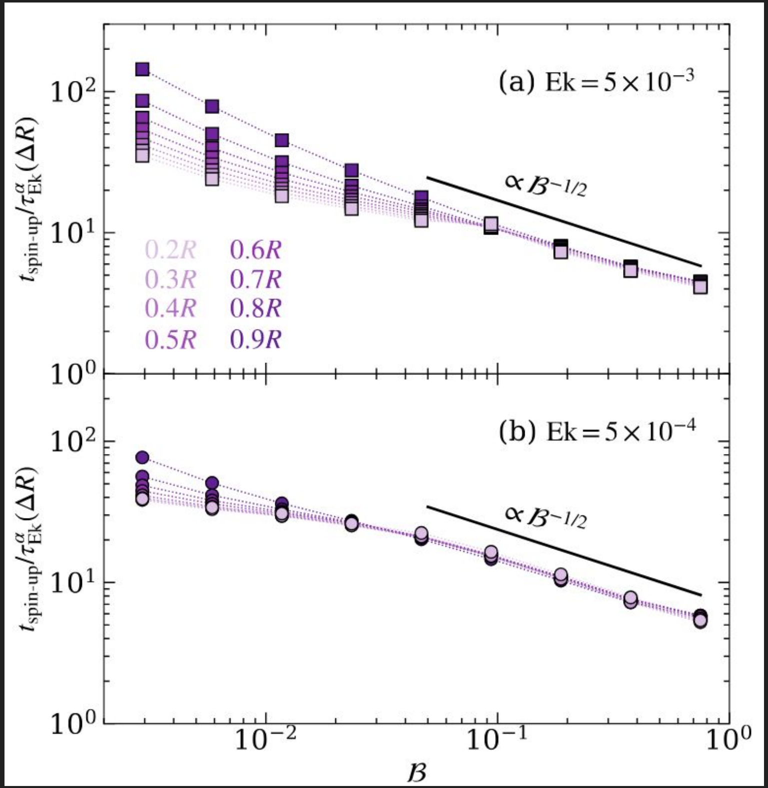

v.graber@herts.ac.uk